



**HAL**  
open science

## Transport mechanisms in MgO/GaAs(001) delta-doped junctions

S. Le Gall, Bruno Lépine, Gabriel Delhaye, Guy Jézéquel, Pascal Turban,  
Philippe Schieffer

► **To cite this version:**

S. Le Gall, Bruno Lépine, Gabriel Delhaye, Guy Jézéquel, Pascal Turban, et al.. Transport mechanisms in MgO/GaAs(001) delta-doped junctions. Applied Physics Letters, 2011, 98 (11), pp.112108. 10.1063/1.3567948 . hal-00732777

**HAL Id: hal-00732777**

**<https://hal.science/hal-00732777v1>**

Submitted on 13 Mar 2020

**HAL** is a multi-disciplinary open access archive for the deposit and dissemination of scientific research documents, whether they are published or not. The documents may come from teaching and research institutions in France or abroad, or from public or private research centers.

L'archive ouverte pluridisciplinaire **HAL**, est destinée au dépôt et à la diffusion de documents scientifiques de niveau recherche, publiés ou non, émanant des établissements d'enseignement et de recherche français ou étrangers, des laboratoires publics ou privés.

## Transport mechanisms in MgO/GaAs(001) delta-doped junctions

S. Le Gall, B. Lépine, G. Delhaye, G. Jézéquel, P. Turban, and P. Schieffer<sup>a)</sup>  
*Equipe de Physique des Surfaces et Interfaces, Institut de Physique de Rennes, UMR URI-CNRS 6251,  
 Université de Rennes, 1, F-35042 Rennes Cedex, France*

(Received 26 January 2011; accepted 28 February 2011; published online 17 March 2011)

The transport mechanisms through MgO ultrathin layers (0.5–1.2 nm) deposited on n-type doped GaAs(001) layers have been studied. In order to favor field emission (FE) across the junctions, a high doping concentration layer in vicinity of the semiconductor surfaces has been included. Varying doping concentration of the underlying GaAs layer we find that the dominant transport mechanism is either the variable-range hopping mechanism or a thermionic emission-like process instead of the FE process. The observation of such mechanisms can be explained by the fact that during the MgO deposition, defect states are introduced in the semiconductor band gap. © 2011 American Institute of Physics. [doi:10.1063/1.3567948]

Control and detection of electrical spin injection between ferromagnetic metallic electrodes and semiconductor is one of the main challenges for the future development of semiconductors-based spintronics devices.<sup>1</sup> In order to solve the problem of the conductivity mismatch between the ferromagnetic metal (FM) and the semiconductor,<sup>2</sup> a spin-dependent interface resistance such as a tunnel barrier must be inserted between the two materials.<sup>3,4</sup> Using optical detection measurements, Jiang *et al.*<sup>5</sup> have shown that a CoFe/MgO tunnel spin injector can provide a high polarization of electrons in a GaAs-based structure. Thus the FM/MgO electrode appears as an interesting candidate to realize electrical spin injection-detection in semiconductor-based devices. However, electrical measurements demonstrate that the resistance-area (RA) product for FM/MgO(0.6 nm)/GaAs(001) (Ref. 6) or FM/MgO(1 nm)/Al<sub>0.2</sub>Ga<sub>0.8</sub>As(001) (Ref. 7) systems, in which an highly doped layer in vicinity of MgO/semiconductor interface is placed, are much larger than the optimum RA product to observe a spin-valve magnetoresistance effect in two-contact devices.<sup>4</sup>

In order to determine the origin of the interface resistance in these junctions we have studied the conduction mechanisms that take place through MgO/GaAs n-type doped structures which have been especially designed to favor the field emission (FE) process (as it was done in the works reported in Refs. 6 and 7) and for MgO thicknesses between 0.5 and 1.2 nm. We find that the dominant transport mechanism is either the variable-range hopping (VRH) conduction or a thermionic emission-like (TE-like) process. The appearance of such mechanisms can be explained by the fact that defect states are introduced during the MgO deposition in the semiconductor band gap at a depth of several tens of nanometers from the MgO/GaAs interface. These defects are in addition to interface states existing at the MgO/GaAs(001) interface.<sup>8</sup>

The delta-doped structures were grown by molecular beam epitaxy (MBE) GaAs(001) substrate in a RIBER 2300 chamber equipped with conventional effusion cells. A 0.5–0.8 μm thick GaAs buffer layer doped at 6 × 10<sup>18</sup> or 5 × 10<sup>16</sup> Si atoms cm<sup>-3</sup>, was grown on heavily doped n-GaAs

substrate (3 × 10<sup>18</sup> cm<sup>-3</sup>) at 580 °C, after which the Ga and Si cells were closed and the substrate temperature was lowered to 500 °C, the As<sub>4</sub> flux was maintained.<sup>9</sup> The Si cell was opened to provide a two-dimensional concentration of 5 × 10<sup>12</sup> Si atoms cm<sup>-2</sup> in the delta-doped layer. The substrate temperature of 500 °C for the growth of the delta-doped layers was chosen to limit Si spreading and segregation effects.<sup>10</sup> Next keeping the Si cell opened and a substrate temperature of 500 °C, a GaAs cap layer of 2.5 nm in thickness was grown. This sequence was repeated five times that allowed to obtain a Si mean doping concentration of 2 × 10<sup>19</sup> cm<sup>-3</sup> in the first 14 nm underneath the GaAs(001) surface. Solving numerically the Poisson's equation with the Fermi energy ( $E_F$ ) located 0.8 eV below the conduction band minimum at the GaAs surface we found that at equilibrium the carriers depletion layer was 4 nm.<sup>11</sup> The MgO layers between 0.5 and 1.2 nm were then deposited at room temperature (RT) by evaporation of high purity MgO powder at approximately 0.6 Å/min under an O<sub>2</sub> atmosphere of 5 × 10<sup>-7</sup> Torr on an As-rich GaAs(001)-(2 × 4) surface. Finally, the 30 nm thick Au metal contacts between 0.25 and 0.50 mm in diameter were deposited *in situ* at RT from an effusion cell using a shadow mask. More details about the preparation of the MgO/GaAs(001) samples can be found elsewhere.<sup>12</sup> The current-voltage measurements were obtained using either a Keithley 2182A nanovoltmeter or Keithley 617 electrometer in the dark for temperatures between 80 and 380 K. For Au contacts directly deposited on delta-doped GaAs(001) surface and with a buffer layer doped at 5 × 10<sup>16</sup> cm<sup>-3</sup>, we found that at RT the specific contact resistance related to metal-semiconductor contact lied below 1 × 10<sup>-8</sup> Ω m<sup>2</sup>, the sensitivity threshold of our experimental setup. It was shown by Schubert *et al.*<sup>13</sup> that for similar structures the specific contact resistances lied in the 10<sup>-10</sup> Ω m<sup>2</sup> range.

Figure 1 shows the evolution of the total resistance ( $R_T$ ) of junctions with a buffer layer doped at 6 × 10<sup>18</sup> cm<sup>-3</sup> measured at the applied voltage ( $V_a$ ) of 10 mV and at RT as a function of the inverse contacts area for MgO thicknesses of 0.5, 0.8, and 1.2 nm. Here, because of the strong doping concentration of the semiconductor structure, the spreading resistance of the semiconductor substrate and resistance of the GaAs epitaxial layer have negligible contributions to the

<sup>a)</sup>Author to whom correspondence should be addressed. Electronic mail: philippe.schieffer@univ-rennes1.fr.

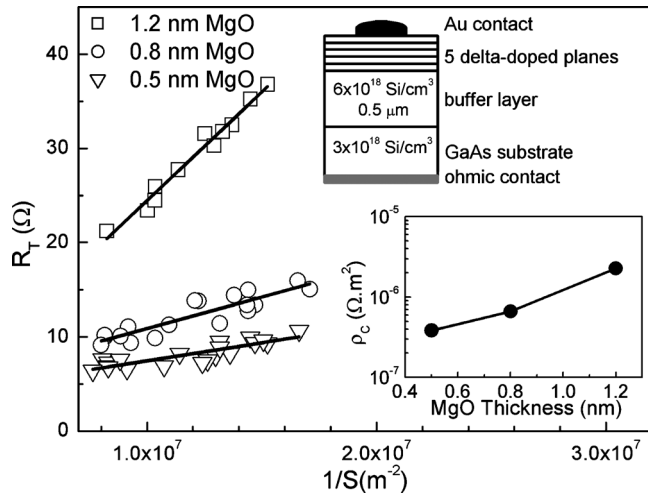


FIG. 1. Measured total resistance  $R_T$  as a function of  $1/S$  for various MgO layers deposited on a GaAs(001) delta-doped layer with a buffer layer doped at  $6 \times 10^{18} \text{ cm}^{-3}$  (symbols) compared to the linear fitting curves (solid lines). Also shown is the scheme of the junction used for the  $J-V_a$  measurements. The inset shows the evolution of  $\rho_C$  as a function of the MgO thickness in semi-logarithmic representation.

total resistance. According to the works of Cox and Strack,<sup>14</sup> the total resistance then can be decomposed as follows:

$$R_T = R_0 + \rho_C/S, \quad (1)$$

where  $R_0$  is the sum of the back-side and probe resistances that do not depend on the contact area  $S$  and  $\rho_C$  is the specific contact resistance. The curves in Fig. 1 are linear and the  $\rho_C$  values extracted from these curves are shown as a function of the MgO thickness in semilogarithmic representation in the inset of Fig. 1. Using the Simmons' model<sup>15</sup> we find that the RA product calculated for a metal/MgO/metal structure with an oxide thickness of 1.2 nm, an electron barrier height of 1.5 eV and an effective mass of  $0.4m_e$  (Ref. 16) lies below  $10^{-10} \text{ } \Omega \cdot \text{m}^2$ . Such a value is much smaller than the  $\rho_C$  values shown in the inset of Fig. 1. This demonstrates that for our Au/MgO/GaAs delta-doped structures the main contribution to the contact resistance does not come from the electrical resistance of the oxide tunnel barrier.

The current density ( $J$ ) as a function of  $V_a$  for an oxide thickness of 1.2 nm and for various temperatures is shown in Fig. 2(a). An enlarged view of the  $J-V_a$  characteristics around  $V_a=0$  V are given in the inset of the figure. The junction shows an Ohmic-like behavior for  $V_a$  values close to 0 V. Considering the theory of tunneling through Schottky barriers developed by Padovani and Stratton<sup>17</sup> we expect that in our degenerate semiconductor structures the FE mechanism dominates the transport at zero-bias over the whole temperature range (80–380 K).<sup>18</sup> If the current flow across the junctions is governed by the FE, the contact resistance should be weakly dependent on the temperature. Instead, we observe a strong temperature dependence of the characteristics slope that demonstrates that the mechanism involved in the charge transport is thermally activated. Actually, the temperature dependence of the experimental conductance ( $G$ ) around  $V_a=0$  V can be explained through the VRH model proposed by Mott.<sup>19,20</sup> In the VRH mechanism the electrons can move among localized states with energies near the Fermi energy via a phonon-assisted tunneling process with

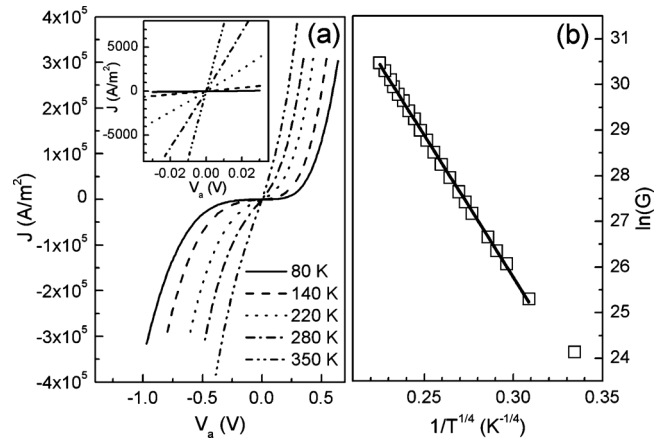


FIG. 2. (a)  $J-V_a$  characteristics for an MgO thickness of 1.2 nm for various temperatures. The inset shows an enlarged view of the Ohmic-like  $J-V_a$  characteristics around  $V_a=0$  V. (b) Logarithm of the experimental conductance at  $V_a=0$  V as a function of  $1/T^{1/4}$  (square) compared to the linear fitting curve (solid line).

the hopping distance increasing with decreasing temperature. The VRH conductance obeys the relationship,

$$G_{\text{VRH}} = G_0 \exp[-(T_0/T)^p], \quad \text{with } T_0 = \beta/[kN(E_F)\xi^3], \quad (2)$$

where  $p=1/4$  for a three-dimensional (3D) system,  $k$  is the Boltzmann's constant,  $\beta$  is a dimensionless constant,  $\xi$  is the wave-function localization radius of the hopping center and  $N(E_F)$  is the density of the localized states (considered as constant in the Mott model) at the Fermi level. As it can be seen in Fig. 2(b), the plot of  $\ln(G)$  versus  $T^p$  with  $p=1/4$  yields a linear curve over the whole temperature range suggesting that the conduction is due to the 3D VRH mechanism. As this behavior is also observed for an oxide thickness of 0.5 nm we conclude that the hopping processes occur among defect states located in the GaAs band gap at the Fermi energy and distributed in the depth of the GaAs layer. Besides, no hopping mechanisms have been detected with intimate Au/GaAs contacts. Therefore, these defect states are introduced in the GaAs layer during the MgO deposition. From a linear fitting of the curve in Fig. 2(b), we obtain  $T_0^{1/4} \approx 62 \text{ K}^{1/4}$  and taking  $\xi=1$  nm and  $\beta=21$ <sup>20</sup> we find that  $N(E_F)=1.6 \times 10^{19} \text{ states/eV/cm}^3$ . For the other MgO thicknesses we extract a similar value for the density of states at the Fermi level ( $\sim 1 \times 10^{19} \text{ states/eV/cm}^3$ ). Considering the GaAs band bending near the MgO/GaAs interface we conclude that the defect states involved in the VRH mechanism must be located in the upper-half part of the band gap. As will be discussed below, other defect states are present in the GaAs band gap. Note that the VRH mechanism can be observed only if a strong change exists in the potential profile, close to the semiconductor surface, induced by the MgO deposition. A phenomenon like a compensation effect allows to explain this change.

Figure 3(a) shows the  $|J|-V_a$  characteristics in semilogarithmic representation for a structure with a buffer layer doped at  $5 \times 10^{16} \text{ cm}^{-3}$ , an MgO thickness of 1.2 nm and for various temperatures. The  $J-V_a$  characteristics that exhibit a rectifying behavior over the whole temperature range closely resemble those obtained by Shashkin *et al.*<sup>21</sup> for metal-semiconductor junctions in which only one delta-doped

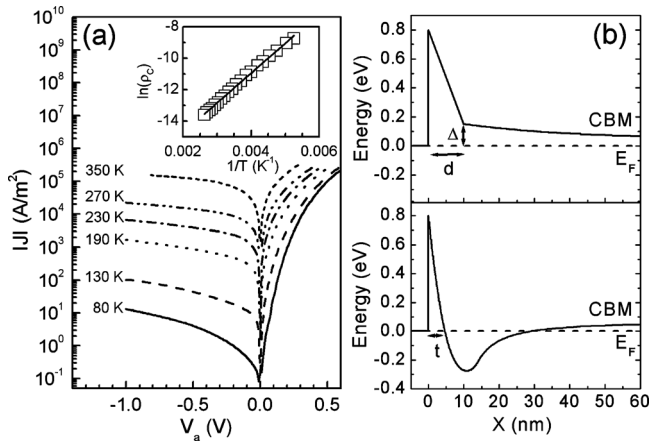


FIG. 3. (a)  $|J|$ - $V_a$  characteristics for an MgO film of thickness 1.2 nm deposited on a GaAs(001) delta-doped layer with a buffer layer doped at  $5 \times 10^{16} \text{ cm}^{-3}$  for various temperatures. The inset gives the corresponding evolution of the  $\ln(\rho_C)$  as a function of  $1/T$  compared to the linear fitting curve (solid line). The quantity  $\rho_C$  is extracted from the  $J$ - $V_a$  characteristics around 0 V. (b) Bottom profile shows the calculated energy-band diagram of a GaAs(001) delta-doped layer with a buffer layer doped at  $5 \times 10^{16} \text{ cm}^{-3}$  at equilibrium and at 300 K. Top profiles corresponds to a schematic energy-band diagram of a GaAs(001) delta-doped layer with a buffer layer doped at  $5 \times 10^{16} \text{ cm}^{-3}$  after the MgO deposition. This profile is deduced from our analysis of the  $J$ - $V_a$  characteristics. CBM is the GaAs conduction-band-minimum and  $X$  is the coordinate normal to the GaAs surface/interface ( $X=0$  corresponds to the position of the interface).

plane is placed near the semiconductor surface at a distance  $d$ . In their work, Shashkin and Murel,<sup>22</sup> taking into account the field and thermionic-FE as well as the effect of the image force on the barrier height lowering, formulated an analytical expression for the current and found that their experimental data could be reproduced through a TE-like model. The schematic energy-band diagram considered in their model is shown as the top profile in Fig. 3(b). According to their approach, the specific contact resistance  $\rho_C$  for a low-barrier diode must be proportional to  $\exp[\Delta/(kT)]$ , where  $\Delta$  is the zero-bias effective barrier height for electrons [the quantity  $\Delta$  is defined in Fig. 3(b)]. We find that for temperatures between 190 and 380 K the plot of  $\ln(\rho_C)$  as a function of  $1/T$  varies linearly, therefore demonstrating that the TE-like process is the dominant mechanism in our junction: the linear fitting of the experimental points [inset of the Fig. 3(a)] gives  $\Delta=0.16 \text{ eV}$ .

The energy-band diagram of our delta-doped n-type metal-semiconductor junction, with a buffer layer doped at  $5 \times 10^{16} \text{ cm}^{-3}$  calculated at 300 K,<sup>11</sup> shows a potential well filled with free electrons [bottom profile in Fig. 3(b)]. In such a structure the tunnel transport through the triangular barrier with a thickness  $t=4 \text{ nm}$  is expected to dominate the charge transport for low voltages. Thus the current-voltage characteristics should be linear, as it was observed by Schubert *et al.*<sup>13</sup> for a metal-semiconductor junction with five highly delta-doped planes placed near the semiconductor surface, and weakly dependent on the temperature. In the presence of MgO such a behavior is not observed and from the preceding analysis we can conclude that the semiconductor energy-band diagram now resembles the top profile in Fig. 3(b). This

result suggests that the MgO deposition on the GaAs surface causes an increase in the extension of the carrier depletion layer and leads to the disappearance of the potential well; this tends to reduce the charge flow by the FE mechanism and consequently makes possible the observation of the TE-like process. A partial compensation effect related to the introduction in the GaAs band gap of negatively charged defects with a concentration comparable or higher than that of the Si atoms in the delta-doped layer therefore must take place.

In conclusion, we have found that the carrier transport across Au/MgO/GaAs(001) n-type doped junctions, where a high doping concentration layer close to the semiconductor surfaces has been included, is dominated either by the VRH mechanism or a TE-like process. The observation of these mechanisms is linked to the presence of defect states in the semiconductor band gap, which are introduced in vicinity of the MgO/GaAs interface during the MgO deposition. The detailed study of the defects properties is currently in progress.

This work was supported by the French Agence Nationale pour la Recherche (MOMES) and the Region Bretagne.

- <sup>1</sup>I. Žutić, J. Fabian, and S. Das Sarma, *Rev. Mod. Phys.* **76**, 323 (2004).
- <sup>2</sup>G. Schmidt, D. Ferrand, L. W. Molenkamp, A. T. Filip, and B. J. van Wees, *Phys. Rev. B* **62**, R4790 (2000).
- <sup>3</sup>E. I. Rashba, *Phys. Rev. B* **62**, R16267 (2000).
- <sup>4</sup>A. Fert and H. Jaffrès, *Phys. Rev. B* **64**, 184420 (2001).
- <sup>5</sup>X. Jiang, R. Wang, R. M. Shelby, R. M. Macfarlane, S. R. Bank, J. S. Harris, and S. S. P. Parkin, *Phys. Rev. Lett.* **94**, 056601 (2005).
- <sup>6</sup>T. Inokuchi, T. Marukame, M. Ishikawa, H. Sugiyama, and Y. Saito, *Appl. Phys. Express* **2**, 023006 (2009).
- <sup>7</sup>J. C. Le Breton, H. Saito, S. Yuasa, and K. Ando, *Appl. Phys. Lett.* **94**, 152101 (2009).
- <sup>8</sup>J. C. Le Breton, S. Le Gall, G. Jézéquel, B. Lépine, P. Schieffer, and P. Turban, *Appl. Phys. Lett.* **91**, 172112 (2007).
- <sup>9</sup>To avoid the formation of highly resistive layer at interface between the buffer layer doped at  $5 \times 10^{16} \text{ cm}^{-3}$  and the substrate (Ref. 23), a 0.4  $\mu\text{m}$  thick GaAs layer doped at  $1.5 \times 10^{18} \text{ cm}^{-3}$  was first grown on GaAs substrate.
- <sup>10</sup>E. F. Schubert, *J. Vac. Sci. Technol. A* **8**, 2980 (1990).
- <sup>11</sup>L.-H. Tan, G. L. Snider, L. D. Chang, and E. L. Hu, *J. Appl. Phys.* **68**, 4071 (1990).
- <sup>12</sup>Y. Lu, J. C. Le Breton, P. Turban, B. Lépine, P. Schieffer, and G. Jézéquel, *Appl. Phys. Lett.* **88**, 042108 (2006).
- <sup>13</sup>E. F. Schubert, J. E. Cunningham, W. T. Tsang, and T. H. Chiu, *Appl. Phys. Lett.* **49**, 292 (1986).
- <sup>14</sup>R. H. Cox and H. Strack, *Solid-State Electron.* **10**, 1213 (1967).
- <sup>15</sup>J. G. Simmons, *J. Appl. Phys.* **34**, 1793 (1963).
- <sup>16</sup>W. H. Butler, X.-G. Zhang, T. C. Schulthess, and J. M. MacLaren, *Phys. Rev. B* **63**, 054416 (2001).
- <sup>17</sup>F. A. Padovani and R. Stratton, *Solid-State Electron.* **9**, 695 (1966).
- <sup>18</sup>To calculate the range of temperature over which our junction exhibits FE an electron Schottky barrier height of 0.8 eV and a doping concentration of  $2 \times 10^{19} \text{ cm}^{-3}$  have been considered.
- <sup>19</sup>N. F. Mott and E. A. Davis, *Electronic Processes in Non-Crystalline Materials* (Clarendon, Oxford, 1979), p. 32.
- <sup>20</sup>B. I. Shklovskii and A. L. Efros, *Electronic Properties of Doped Semiconductors* (Springer, New York, 1984), p. 208.
- <sup>21</sup>V. I. Shashkin, A. V. Murel, V. M. Daniltsev, and O. I. Khrykin, *Semiconductors* **36**, 505 (2002).
- <sup>22</sup>V. I. Shashkin and A. V. Murel, *Semiconductors* **38**, 554 (2004).
- <sup>23</sup>Y. Iimura, T. Shiraishi, H. Takasugi, and M. Kawabe, *J. Appl. Phys.* **61**, 2095 (1987).